

Controlling Quantum Transport by State Synthesis in Ion Traps

Juan F. Poyatos¹ and Gonzalo García de Polavieja²

¹Centre for Quantum Computation, Clarendon Laboratory, Parks Road, Oxford OX1 3PU, United Kingdom

²Physical and Theoretical Chemistry Laboratory, South Parks Road, Oxford OX1 3QC, United Kingdom

(Received 6 April 1999)

A procedure to control the quantum transport between classical regions is proposed. The scheme exploits the ability to synthesize arbitrary motional states in ion traps. Quantum barriers and passages to transport can be created selecting the relevant frequencies. This technique is then applied to stabilize the quantum motion onto classical structures or alter the dynamical tunneling in nonintegrable systems.

PACS numbers: 32.80.Pj, 03.65.Bz, 03.65.Sq

Systems for which predictions can be made using classical mechanics can show quantum mechanical properties under suitable experimental conditions. The observables measured can be of a nonclassical class as in Bell experiments. States can also be chosen to deviate from classical behavior, an idea that we will exploit in the present Letter. Despite this, the study of the classical dynamics continues to be a guide to provide insight into the nature of quantum systems, specially in the case of atomic and molecular physics [1]. More recently, a new class of experiments for which Hamiltonians can be engineered and detailed properties can be monitored have allowed us to apply this relation in more detail. Cold atoms experiments have shown the possibility of inducing quantum dynamics with a particularly appealing classical limit, the δ -kicked rotor. These experiments observed dynamical localization, accelerator modes, and only recently the effect of noise and dissipation [2]. In addition there have been theoretical proposals of experimental configurations in ion traps to study dynamical localization [3], revivals [4], and state sensitivity [5,6].

In this Letter we show how to control and monitor quantum transport between two or more classical regions in an ion trap. The control is achieved not only by engineering the Hamiltonian but most importantly by state synthesis. To monitor the relevant effects we use tomography and simpler alternative techniques. Trapped ions' advantages to both control and monitor have already been used for the study of other aspects of quantum systems, such as the quantum Zeno effect [7], possible nonlinear variants of quantum theory [8], reservoir engineering [9], and quantum computation [10].

To see the relative contribution of the classical backbone and the purely quantum effects consider the Q distribution that is measured in tomography [11]. Its continuity equation is of the form [12]

$$\frac{\partial Q}{\partial t} + \{Q, H\} + Z(V, Q, t, \hbar) = 0, \quad (1)$$

with $Q(\alpha; t) = |\langle \alpha | \Psi(t) \rangle|^2$, being $|\alpha\rangle$ a coherent state, V the potential, and $\{, \}$ the classical Poisson bracket. This continuity equation is the classical Liouville equa-

tion plus a quantum term $Z(V, Q, t, \hbar)$ given by $Z = -\frac{2}{\hbar} \text{Im}\{\langle \Psi | \alpha \rangle V(x/2 + i\hbar\partial/\partial p) \langle \alpha | \Psi \rangle\}$. An ideal experimental setup to study the relation between quantum and classical dynamics would then have the possibility to control all three dependencies of Z , i.e., the potential, the quantum state, and an effective Planck constant. Moreover, it should be possible to have measurable quantities showing the relative importance of classical and quantum contributions, e.g., the Q distribution itself. All of the above conditions can be fulfilled in the case of a harmonically trapped ion. This is possible due to the interaction between the internal (electronic) and external (vibrational) degrees of freedom of the ion by means of laser pulses in resonant and nonresonant regimes [13].

Consider the regime where both the classical Liouville and the quantum terms in the continuity equation in (1) are relevant. The quantum contribution to the transport is state dependent and the final flow is diverted from the classical flow by an amount that depends on the quantum state. We first pick out the classical backbone structure and then study how to manipulate the quantum transport depending on the synthesized state. We need to construct a family of Hamiltonians that have regular, mixed, or chaotic phase space. In the trapped ion setup we make use of the harmonic delta kicked Hamiltonian [5], describing a harmonic oscillator periodically perturbed by nonlinear position dependent delta kicks. We consider a single trapped ion in a harmonic potential [13] (i.e., a linear ion trap) with two internal levels $|e\rangle$ and $|g\rangle$ with transition frequency ω_0 interacting with a time dependent laser pulse of near-resonant light of frequency ω_L which is rapidly and periodically switched. For sufficiently large detuning $\delta = \omega_0 - \omega_L$ the excited state amplitude can be adiabatically eliminated. Assuming that the minimum of the trap potential coincides with an antinode of the off-resonant laser standing wave, the Hamiltonian reads [5,14]

$$H = H_0 + K[\cos(2k_L x) + 1]|g\rangle\langle g| \sum_{n=-\infty}^{\infty} \delta(t - n\tau), \quad (2)$$

where H_0 is the harmonic oscillator Hamiltonian, $k_L = 2\pi/\lambda$ is the laser wave number, τ is the time between

kicks, and $K = \sqrt{\pi} \hbar \sigma \Omega^2 / 8\Delta$ is the kick strength. Here σ is the Gaussian laser beam width, Ω is the Rabi frequency, and Δ is the laser detuning. A particularly important parameter is the so-called Lamb-Dicke parameter $\eta = k_L \sqrt{\hbar / 2m\nu}$, where ν is the oscillator frequency and m is the mass. An effective $\hbar_{\text{eff}} = 2\eta^2/\pi$ is obtained after rescaling to a dimensionless Hamiltonian [14]. Thus when varying η by changing the trap frequency the \hbar_{eff} is modified.

In the following the relevance of the classical backbone is shown by predicting the time-averaged quantum Q function by means of classical theorems. We write the potential for a phase space region as $V = V_0 + V_1$, with V_0 and V_1 the unperturbed and perturbed potentials that in general have different phase space topologies. The time-averaged dynamics of an initially synthesized motional Fock state is shown to be predicted from knowledge of the classical solution for V_0 and the Kolmogorov-Arnold-Moser (KAM) and the Poincaré-Birkhoff theorems [15]. These two theorems in conjunction mean that, increasing the perturbation V_1 , the phase space tori break in increasing irrationality values of the ratio of their winding numbers $r = \omega_1/\omega_2$ with ω_1 and ω_2 the two frequencies of a given torus [16]. When the winding number is sufficiently close to the rational number l/s the torus breaks into alternative js stable and unstable points, with j, l, s integers [15].

Figure 1(a) shows the classical stroboscopic map for V_0 . Following the values of the winding number increasing the perturbation we determine which torus is breaking first. We thus predict the averaged quantum behavior with total potential $V = V_0 + V_1$ using only the classical information from the values of the winding numbers with $V = V_0$ and the classical theorems. Then a $|n\rangle = |7\rangle$ Fock state is predicted to have an averaged Q function with four maxima (minima) on the classically stable (unstable) points when increasing the perturbation of the system. Figure 1(b) shows the time-averaged Q function

$$Q_T = \lim_{M \rightarrow \infty} \frac{1}{M\tau} \sum_{m=0}^{M-1} Q(m\tau) = \sum_{\mu} |\langle \alpha | \mu \rangle|^2 |\langle \Psi | \mu \rangle|^2, \quad (3)$$

with $|\mu\rangle$ the Floquet states fulfilling $\hat{U}(\tau)|\mu\rangle = e^{-i\epsilon_{\mu}}|\mu\rangle$, where $\hat{U}(\tau)$ is the time evolution operator referring to one period τ and Ψ is a given initial state. The four predicted maxima are clear in this figure. Figure 1(c) displays the Q function averaged at three consecutive times, as it could be measured experimentally using three tomographic measurements [11] showing the same structure. The classical stroboscopic map for the perturbed case in Fig. 1(d) shows clearly that Q_T reveals the classical backbone in many details. Any other Fock state prepared would scan in the same way different structures of this or alternative classical maps.

We now propose to control the relative relevance of the quantum and classical terms in (1) by state syn-

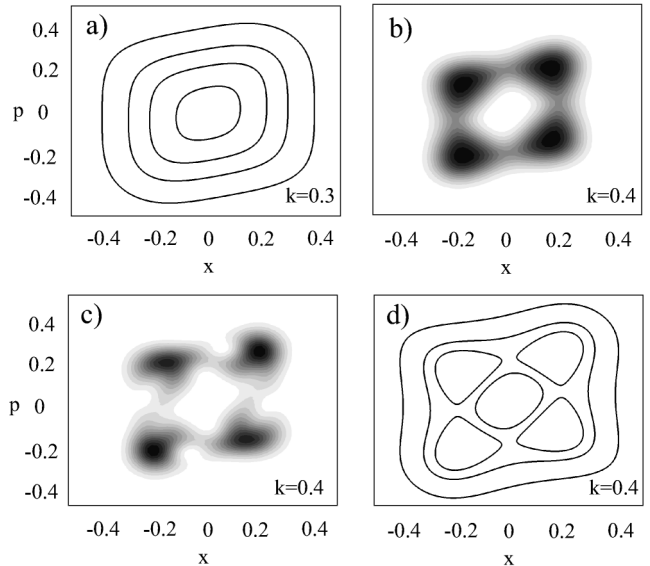


FIG. 1. (a) Stroboscopic classical map with $k = 0.3$. The rational number to which the winding number approaches is $1/4$ for the initial condition $(x, p) = (0.22, 0)$. (b) Q_T function with $k = 0.4$ and $\eta = 0.25$ (see text). (c) Q function averaged over three different tomographic measurements after applying 21, 22, and 23 kicks. All parameters are as before. (d) Stroboscopic classical map with $k = 0.4$. $\nu\tau = 1.8$ for all the cases. x and p are in units of λ and $m\nu\lambda$ in all discussions and $k = \sqrt{2} K \eta^2 / \hbar$.

thesis. We want to prepare a state initially localized in a classical region A with a *barrier* or a *passage* for transport to a different classical region B . Take as a starting state a coherent state localized on A , $\phi_A(0)$. Its averaged transport to region B , represented by another state ϕ_B , is given by $P(|\phi_A\rangle, |\phi_B\rangle) = \lim_{M \rightarrow \infty} \frac{1}{M\tau} \sum_{m=0}^{M-1} |\langle \phi_B | \phi_A(m\tau) \rangle|^2$, that we can write as $P(|\phi_A\rangle, |\phi_B\rangle) = \sum_{\mu} |\langle \phi_B | \mu \rangle|^2 |\langle \phi_A(0) | \mu \rangle|^2$ using the Floquet basis. For $P(|\phi_A\rangle, |\phi_B\rangle)$ not to be zero, the states $\phi_A(0)$ and ϕ_B must have nonzero overlap with common Floquet states denoted as $\{|\mu\rangle_{A \cap B}\}$. To form a new state that minimizes, $\varphi_{A'}^{-B}$, or maximizes, $\varphi_{A'}^{+B}$, the transport to region B we eliminate (enhance) from $\phi_A(0)$ the Floquet components $\{\mu_{A \cap B}\}$ as

$$|\varphi_{A'}^{\pm B}\rangle = N_1(|\phi_A(0)\rangle \pm \sum_{\mu_{A \cap B}} r_{\mu} |\mu\rangle \langle \mu | \phi_A(0)\rangle), \quad (4)$$

with $r_{\mu} = 0$ or 1 when the corresponding weight $|\langle \mu | \phi_A \rangle|^2$ is smaller or greater than a value c_{tol} , respectively, and N_1 will be normalization constants from now on. The value c_{tol} is chosen to be the minimum possible subject to the condition that the new region A' is sufficiently close to the initial region of localization A . We propose then the synthesis of the states

$$|\Psi_{A'}^{\pm B}\rangle = N_2 \sum_{n=0}^{n_{\text{exp}}} |n\rangle \langle n | \varphi_{A'}^{\pm B}\rangle, \quad (5)$$

with $\{|n\rangle\}$ the Fock basis and where we consider only an experimentally feasible maximum number of Fock states n_{exp} [17] and amplitudes $\langle n | \varphi_{A'}^{\pm B} \rangle$ chosen to approximate the theoretical state (4).

Some comments are necessary: (a) We could use an initial state localized in region A' slightly bigger than the region A of the minimum uncertainty wave packet or an additional localization in a different region A'' . (b) If we want to modify the transport only to region B and not to other regions C we have to use $r_\mu = 0$ in (4) for the Floquet states that have an important overlap with a state ϕ_C centered on C . (c) The states localized in the regions A , B , and C do not need in general to be minimum uncertainty states.

We now discuss a general case of modified transport properties of a given state and we then study stabilization and modification of dynamical tunneling as two interesting examples. We want to synthesize a state $\Psi_{A'}^{-B}$ initially localized on $(x_A, p_A) = (0.1, 0.2)$ that avoids transport to $(x_B, p_B) = (0.3, 0.3)$. We use coherent states for ϕ_A and ϕ_B and a value $c_{\text{tol}} = 0.001$ so all the Floquet states with important overlap with ϕ_B have $r_\mu = 1$ in (4). An experimentally realizable state with $n_{\text{exp}} = 10$ can be constructed with overlap $|\langle \Psi_{A'}^{-B} | \varphi_{A'}^{-B} \rangle|^2 = 0.9$ to the theoretical state. Despite both wave functions $\langle \alpha | \phi_A \rangle$ and $\langle \alpha | \Psi_{A'}^{-B} \rangle$ being initially localized around A , with $|\langle \phi_A | \Psi_{A'}^{-B} \rangle|^2 = 0.82$, it is clear from Figs. 2(a) and 2(b) that their Q_T functions are very different. The Q_T function for $\Psi_{A'}^{-B}$ shows a clear hole at the location B , in contrast to the minimum uncertainty state ϕ_A . The correlation function $P(m\tau) = |\langle \phi_B | \hat{U}^m(\tau) | \Phi \rangle|^2$ is shown in Fig. 2(c) for $\Phi = \phi_A$ and $\Psi_{A'}^{-B}$, the latter showing a significant decrease. These correlation functions can be measured experimentally by applying a displacement associated to ϕ_B and then measuring the Fock ground state population both steps possible to implement in a trap [18]. Successful results can also be obtained for the state $\Psi_{A'}^{+B}$ that presents a maximum on region B in Q_T ; see Fig. 2(c). Figure 2(d) shows the classical map together with a small black box with an area of effective $\hbar_{\text{eff}} = 2\eta^2/\pi^2 \approx 0.05$. While there is no classical flow between points A and B a Gaussian state manifests quantum transport to B . With the state synthesis procedure just shown we are able to increase or decrease the transport controlling in this way how quantum or classical the state behaves concerning this transport.

Particular instances of the states $\Psi_{A'}^{\pm B}$ are of special relevance. The stabilization of the vibration of the ion can be understood as a modified transport problem. In this case A is the region of localization and B is the rest of the phase space and we are interested in constructing a state $\Psi_{A'}^{-B}$ that we will name for the stabilization case as $\Psi_{A'}^{\text{sta}}$. An alternative way to understand expression (5) for this situation now in terms of the dynamics is given in the following. The autocorrelation function of a typical state $|\langle \phi_A(0) | \phi_A(t) \rangle|^2$ will show an initial

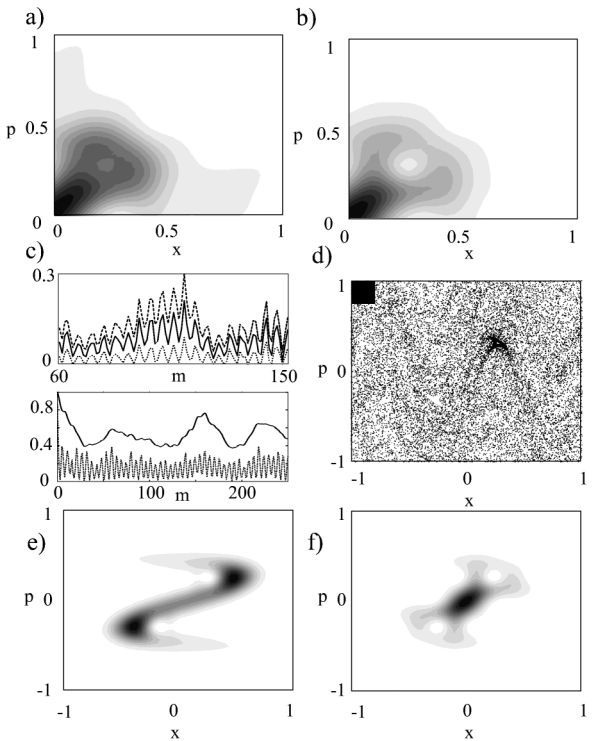


FIG. 2. (a) Q_T function for ϕ_A coherent state. (b) Q_T function for the modified $\Psi_{A'}^{-B}$ state. (c) Upper plot: Correlation function for ϕ_A , $\Psi_{A'}^{-B}$ (dotted line) and $\Psi_{A'}^{+B}$ (dashed line) with ϕ_B . Lower plot: Autocorrelation function for $\Psi_{A'}^{\text{sta}}$ state and ϕ_A coherent state (dotted line). (d) Stroboscopic classical map. The small black box has an area of effective $\hbar_{\text{eff}} = 2\eta^2/\pi^2 \approx 0.05$. (e) Q for an initial coherent state centered at $(x_A, p_A) = (0, 0)$ after two kicks. (f) Q for the stabilized state $\Psi_{A'}^{\text{sta}}$. All figures were obtained with the parameters $k = 2.7$, $\nu\tau = 1.7$, and $\eta = 0.5$.

maximum (however small) at $t_M > 0$. We can now clean the state ϕ_A of the Floquet components that do not contribute to this maximum and therefore create a new state stabilized on A . Note first that a particular Floquet state $|\mu_0\rangle$ can be obtained from the time-dependent vector $|\phi_A(t)\rangle = \sum_\mu |\mu\rangle \langle \mu | \phi_A(0)\rangle \exp(-i\epsilon_\mu t)$ (a solution of the Schrödinger equation *only* for $t = m\tau$) as $|\mu_0\rangle \propto \lim_{T \rightarrow \infty} G_{T,\mu_0}$ with $G_{T,\mu_0} \equiv \int_{-T}^T dt |\phi_A(t)\rangle \exp(i\epsilon_{\mu_0} t)$. A state related to the short term dynamics is then G_{t_M,ω_0} with ω_0 the value of ω that makes $S(\omega) = \int_{-t_M}^{t_M} dt \langle \phi_A(0) | \phi_A(t) \rangle \exp(i\omega t)$ a maximum [19]. This state G_{t_M,ω_0} can then be approximated as

$$|\varphi_{A'}^{\text{sta}}\rangle = N_3 \sum_{\mu_{\text{sta}}} |\mu\rangle \langle \mu | \phi_A(0)\rangle, \quad (6)$$

with μ_{sta} the Floquet eigenfrequencies in the interval $\omega_0 - \frac{\pi}{t_M} < \omega < \omega_0 + \frac{\pi}{t_M}$ with a weight $|\langle \mu | \phi_A(0) \rangle|^2 > a_{\text{sta}}$. The value of a_{sta} is chosen maximum with the requirement that the state $\varphi_{A'}^{\text{sta}}$ has a tolerable localization around A . The state $\Psi_{A'}^{\text{sta}}$ in (5) synthesized to approximate $\varphi_{A'}^{\text{sta}}$ will then show an initial localization around A

because it selects the short term dynamics and will recur continuously to A because it is made of very few selected Floquet states. In fact there are several maxima in $S(\omega)$ and we can choose the value ω_0 with a minimum number of Floquet states maximizing stabilization in this way.

Using this stabilization procedure we have found enhanced localization onto KAM tori, islands of size smaller than the effective \hbar , cantori, or unstable periodic orbits effects [20]. The following example of enhanced localization onto a classical unstable orbit can be realized experimentally. We consider the stroboscopic map in Fig. 2(d). Figure 2(e) shows the Q function for an initial minimum uncertainty state, ϕ_A , after two kicks centered at $(x_A, p_A) = (0, 0)$. The state is spread from an unstable periodic orbit along the unstable manifold. The stabilization is achieved in this case with a state $\Psi_{A'}^{\text{sta}}$ centered on the middle of the chaotic region at $(0, 0)$ with $|\langle \varphi_{A'}^{\text{sta}} | \Psi_{A'}^{\text{sta}} \rangle|^2 = 0.72$ and $n_{\text{exp}} = 12$, a single Floquet state. The stabilization achieved is clearly seen in the measurable autocorrelation function [18]; see Figs. 2(c) and Fig. 2(f) for the Q function of such a stabilized state. This example constitutes a realizable experiment to directly observe a *quantum scar* [21].

As a final example we show how to increase the dynamical tunneling associated to classically forbidden regions, see Fig. 3(a). An initial minimum uncertainty state located at $(x_A, p_A) = (-0.6, 0)$ has dynamical tunneling and contributions from an unstable periodic orbit located at $(x_B, p_B) = (-0.5, 0.3)$. A state (4) eliminating the contributions of B is mainly composed of three Floquet doublets reflecting the oscillations due to quantum tunneling. The autocorrelation function is shown in Fig. 3(b) for a state (5) with $|\langle \varphi_{A'}^B | \Psi_{A'}^B \rangle|^2 = 0.85$. This can be measured by applying displacements associated to the initial regions of localization or more directly by inverting the unitary process which created the initial state. An example of stabilization in this case is choosing a state made of a single doublet where $|\langle \varphi_{A'}^{\text{sta}} | \Psi_{A'}^{\text{sta}} \rangle|^2 = 0.8$. In this case the oscillations due to the tunneling are more clearly reflected. Both states with $n_{\text{exp}} = 25$ since their location in phase space implies higher Fock state contri-

butions than previous cases. Choosing different doublets would give rise to different tunneling times. Finally notice that by increasing n_{exp} , i.e., the overlap to the theoretical state, all features discussed in previous examples will be more dramatically shown [17].

In conclusion, we have presented a method to control quantum transport between classical regions by making use of the ability to synthesize arbitrary states of motion in an ion trap. Within this framework, we have studied the relevance of the classical backbone of a quantum system, the stabilization of motion, and the modification of dynamical tunneling in nonintegrable systems.

G.G.P. acknowledges M.S.S. Child for support. J.F.P. is supported by the European TMR network ERB-4061-PL-95-1412 and thanks M. Baena for helpful discussions.

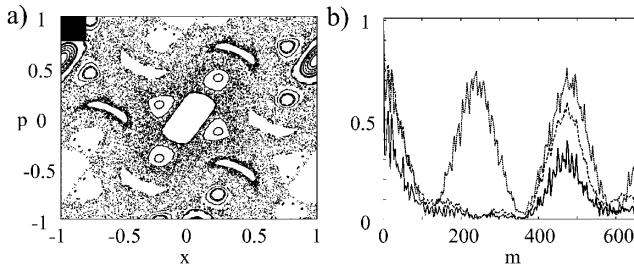


FIG. 3. (a) Stroboscopic classical map with $k = 1.2$ and $\nu\tau = 2\pi/3$. (b) Autocorrelation function for an initial coherent state, Floquet doublet (dotted line), and $|\Psi_{A'}^B\rangle$ state (dashed line). Parameters as before with $\eta = 0.5$. The area of the black box is $\hbar_{\text{eff}} \approx 0.05$.

- [1] A. Peres, *Quantum Theory: Concepts and Methods* (Kluwer Academic Publishers, Dordrecht, 1993).
- [2] F.L. Moore *et al.*, Phys. Rev. Lett. **73**, 2974 (1994); F.L. Moore *et al.*, *ibid.* **75**, 4598 (1997); H. Ammann *et al.*, *ibid.* **80**, 4111 (1998); B. G. Klappauf *et al.*, *ibid.* **81**, 1203 (1998).
- [3] M. El Ghafar *et al.*, Phys. Rev. Lett. **78**, 4181 (1997); G. P. Berman *et al.*, quant-ph/9903063.
- [4] J. K. Breslin *et al.*, Phys. Rev. A **56**, 3022 (1997).
- [5] S. A. Gardiner *et al.*, Phys. Rev. Lett. **79**, 4790 (1997).
- [6] G. G. de Polavieja, Phys. Rev. A **57**, 3184 (1998).
- [7] W. M. Itano *et al.*, Phys. Rev. A **41**, 2295 (1990).
- [8] J. J. Bollinger *et al.*, Phys. Rev. Lett. **63**, 1031 (1989).
- [9] J. F. Poyatos *et al.*, Phys. Rev. Lett. **77**, 4728 (1996).
- [10] C. Monroe *et al.*, Phys. Rev. Lett. **75**, 4714 (1995).
- [11] D. Leibfried *et al.*, Phys. Rev. Lett. **77**, 4281 (1996).
- [12] G. G. de Polavieja, Phys. Lett. A **220**, 303 (1996).
- [13] D.J. Wineland *et al.*, J. Res. Natl. Inst. Stand. Technol. **103**, 259 (1998); Fortschr. Phys. **46**, 363 (1998).
- [14] J. Dalibard and C. Cohen-Tannoudji, J. Opt. Soc. Am. B **2**, 1707 (1985); R. Graham *et al.*, Phys. Rev. A **45**, R19 (1992).
- [15] M. Tabor, *Chaos and Integrability in Nonlinear Dynamics* (John Wiley and Sons, New York, 1989).
- [16] The dynamics associated to the harmonic delta kick is best described in terms of a two-dimensional Poincaré surface of section where only two frequencies are involved.
- [17] Experimentally Fock states have been synthesized up to $n_{\text{exp}} = 16$ ($\eta \sim 0.2$). See D.M. Meekhof *et al.*, Phys. Rev. Lett. **76**, 1796 (1996). However, recent theoretical proposals to prepare arbitrary quantum states work with significantly higher Fock states, e.g., $n_{\text{exp}} = 32$, and higher Lamb-Dicke parameters. These proposals seem to be possible with actual or near future technology. See S. A. Gardiner *et al.*, Phys. Rev. A **55**, 1683 (1997); B. Kneer and C.K. Law, *ibid.* **57**, 2096 (1998).
- [18] J. F. Poyatos *et al.*, Phys. Rev. A **53**, R1966 (1996).
- [19] G. G. de Polavieja *et al.*, Phys. Rev. Lett. **73**, 1613 (1994).
- [20] J. F. Poyatos and G. G. de Polavieja (to be published).
- [21] E. J. Heller, Phys. Rev. Lett. **53**, 1515 (1984).